A SEQUENCED CATALOG OF THE MOON'S LARGEST CRATERS AND BASINS.

Charles J. Byrne, Image Again, 39 Brandywine Way, Middletown, NJ 07748, charles.byrne@verizon.net.

Introduction: The formation ages of individual rock samples from the Moon can be accurately measured but the source of the rocks, where their age was last reset by melting or shock, is often difficult to determine. On the other hand, it is often possible to estimate the sequence of lunar impact features that are large enough to reset the age of rocks. For some purposes, the Sequence Numbers can be used as a surrogate for age.

Two major studies [1, 2] have established sequences for lunar basins (impact features greater than 300 km in diameter). A new study [3] has added 25 large craters in the range of 200 km to 300 km after sequencing 47 basins, inserting the smaller features in the sequence of basins (primarily by relative degradation). As a result, the number of sequenced features has increased to 72, improving the ability to infer historic variations in the rate and size of impacts.

Selection of features: Since study [1], based mostly on Lunar Orbiter images, some basins have been deleted as unlikely and others added, based on new data from later orbiting missions and modeling methods [4, 5]. Some new features revealed by Bouguer gravity data are included in the catalog but 13 features revealed by gravity were examined and found to have been too degraded to be assigned Sequence Numbers.

The Catalog: The basis of the new sequence is a Catalog of the selected craters and basins, collecting data from the Lunar Reconnaissance Orbiter (LRO), GRAIL, and Kaguya, and crater density from study [2].

Example: The parameters of the Orientale Basin:
Age group: EI, Sequence Number, 69
Latitude: -19.6, Longitude: -95.0
Apparent Diameter: 890 km, Rim Crest Diameter: 994 km
Apparent Depth: 4.68 km
Target type: Solid

The image and topography are shown in Figures 1 and 2.

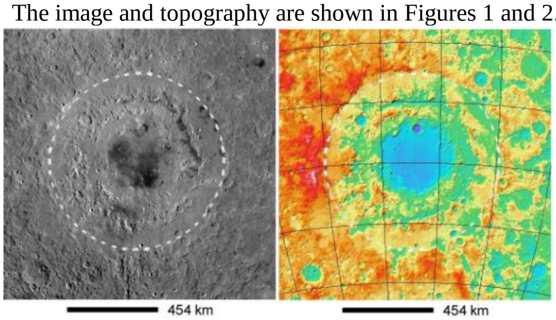

Figure 1 Left: The Orientale Basin, with its Montes Rook rings, ends the Early Imbrian period. **Right:** The outer Montes Rook ring is an unusual feature of the very clear structure of the Orientale Basin. Source: LRO, ASU, [3, Chapter 8].

The radial profile graph and Bouguer gravity anomaly map are shown in Figure 2.

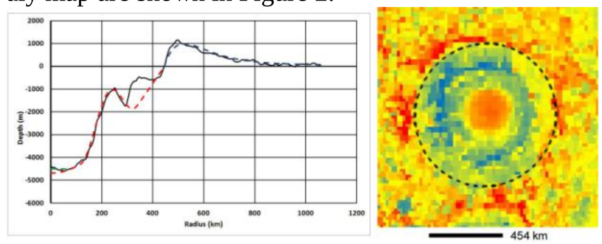

Figure 2 Left: The radial profile [4, 5] shows the extent of the inner and outer Montes Rook. This is the only basin of its size that shows the full depth of the model (dashed line). **Right:** The Bouguer gravity map shows a very high value of Bouguer Anomaly Contrast [6], 726 mGal: the positive anomaly is bounded by the inner Montes Rook, the peak ring of the feature. As usual, outside of the peak ring is a smaller negative anomaly. The edge of the apparent crater is neutral. There is no unique pattern of Bouguer gravity associated with the outer Montes Rook ring. Sources: Radial profile based on Kaguya elevation [7], Bouguer gravity based on GRAIL gravity and LRO elevation [3, Chapter 8].

Sequence Number: The sequence of features is determined by a combination of factors:

- Stratigraphy
- Density of superposed craters more than 20 km in diameter in areas of a feature judged to be free of major degradation by later features [2].
- Relative degradation, especially of the rims and ejecta fields.
- The basins were placed in sequence first and then the large craters were interpolated principally by relative degradation, unless stratigraphy relations were available.

Crater Density graph: Superposed crater density is graphed against Sequence Number in Figure 3.

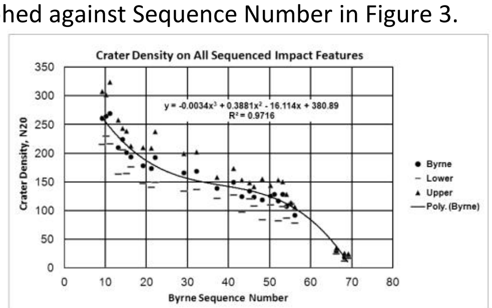

Figure 3: This shows the superposed Crater Density for the entire range of the impact features of this catalog. Points are graphed only if crater densities are available from the Fassett study [2]. The triangles are upper limits and the dashes are lower limits [3, Chapter 2].

The superposed crater density follows a smooth third order polynomial. The R^2 value of 0.97 shows a very high correlation factor between the Sequence Numbers of the catalog with the crater densities of the Fassett study [2}.

Depth vs. Sequence Number: In Figure 4, the rim crest diameter is graphed against the assigned Sequence Number of large basins and craters. The graph shows two interesting regions of large impact features, the Early Heavy Bombardment and the Late Heavy Bombardment. In each case, there is a distinct separation between the larger features and the smaller features.

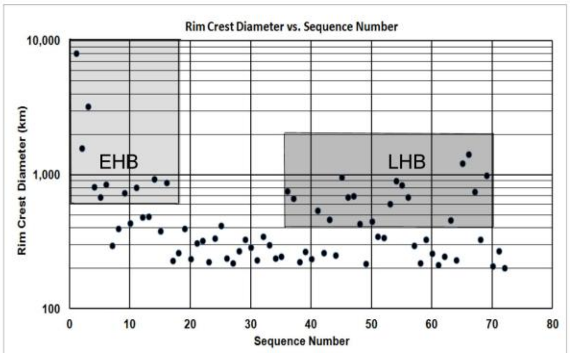

Figure 4: This graph outlines the regions of impact features with relatively large diameters, the Early Heavy Bombardment and the Late Heavy Bombardment. Outside of these two regions, there is a region of smaller features with a gradual reduction of maximum size with Sequence Numbers [3, Chapter 3].

Early Heavy Bombardment (EHB): The EHB starts with the giant basins and gradually declines to a reasonably uniform population and rate of smaller features after the EHB. There is a lack of large craters during the start of the EHB that can be explained as extreme degradation by the cavity, rim, and ejecta field of the giant basins.

Several features have been discovered by their Bouguer gravity anomaly contrast. Some of these are too degraded to be assigned reliable Sequence Numbers. These features probably were degraded by large basins of the EHB. If they could be assigned Sequence Numbers they would extend the sequence interval of the EHB.

Late Heavy Bombardment (LHB): Between the EHB and the LHB, there was an interval of an approximately constant population of large craters. Then, in the LHB, there were a number of basins with diameters more than 400 km, not only larger than the craters but also larger than all but a few small basins. They appear to be from a different population of impactors.

Further, there were intervals of few or even no large craters when there were several basins. It is unlikely that these basins could have such an effect by obscuring the craters: more likely, these LHB basins came in a very short period of time, perhaps sporadically.

Conclusions: The EHB basins were very much larger than the large craters. At least the first four of them obscured the topography of some of these craters, even though they were detected by GRAIL through their Bouguer gravity anomaly. The actual diameter distribution of these impactors was probably typical of such distributions.

There was an interval of Sequence Numbers (and an uncertain period of time), where the rate and size distribution of large craters appeared to be relatively uniform.

Then, during the LHB, a numerous population of large impactors appeared during a relatively short period of time. After the LHB, the impact rate dropped precipitously. There were no basins and only three large craters after the Orientale Basin, Sequence Number 69.

This interesting pattern might provide a clue to help decisions between the Nice model [8] and other recent models of disruption of the early solar system [9].

References:

[1] Wilhelms, D. E. (1987) The Geologic History of the Moon, USGS Professional Paper 1348.

[2] Fassett, C. I., Head, J. W., Kadish, S. J., Mazarico, E., Neumann, G. A., Smith, D. E., and Zuber, M. T. (2012) Lunar Impact Basins: Stratigraphy, sequence and ages from superposed impact crater populations measured from Lunar Orbiter Laser Altimeter (LOLA) data, JGR, Vol. 117.

[3] Byrne, C. J (2015) The Moon's Largest Craters and Basins: Images and Topographic Maps from LRO, GRAIL, and Kaguya, Springer, doi 10.1007/978-3-319-22032-1.

[4] Byrne, C. J. (2008) A Large Basin on the Near Side of the Moon, Earth, Moon, and Planets, v. 101, p. 153–188, 2007, doi:10.1007/s11038-007-9225-8, 2007 (on line), 2008 (print).

[5] Byrne, C. J. (2013) The Moon's Near Side Megabasin and Far Side Bulge, Springer, doi10.1007/978-1-4614-6949-0.

[6] Neumann, G. A, et al. (2015) Lunar Impact Basins Revealed by the Gravity Recovery and Interior Laboratory (GRAIL) mission, Science Advances, 2015.

[7] Japan Aerospace Exploration Agency (JAXA), Result of Kaguya, (1) The global 1 degree grid topographic data, website: http://www.selene.jaxa.jp/en/science/LALT/The_lunar_topographic_data_e.htm.

[8] Bottke, W. F. (2012) The great Archean bombardment, LPSC 2012, Abstract #4036.

[9] Kaib, N. A. and Chambers, J. E. (2015) The fragility of the terrestrial planets during a giant planet instability, http://mnras.oxfordjournals.org/content/455/4/3561.